iScience, Volume *27*

Supplemental information

Multivalent GU-rich oligonucleotides sequester TDP-43 in the nucleus by inducing high molecular weight RNP complexes

Xi Zhang, Tanuza Das, Tiffany F. Chao, Vickie Trinh, Rogger P. Carmen-Orozco, Jonathan P. Ling, Petr Kalab, and Lindsey R. Hayes

Figure S1

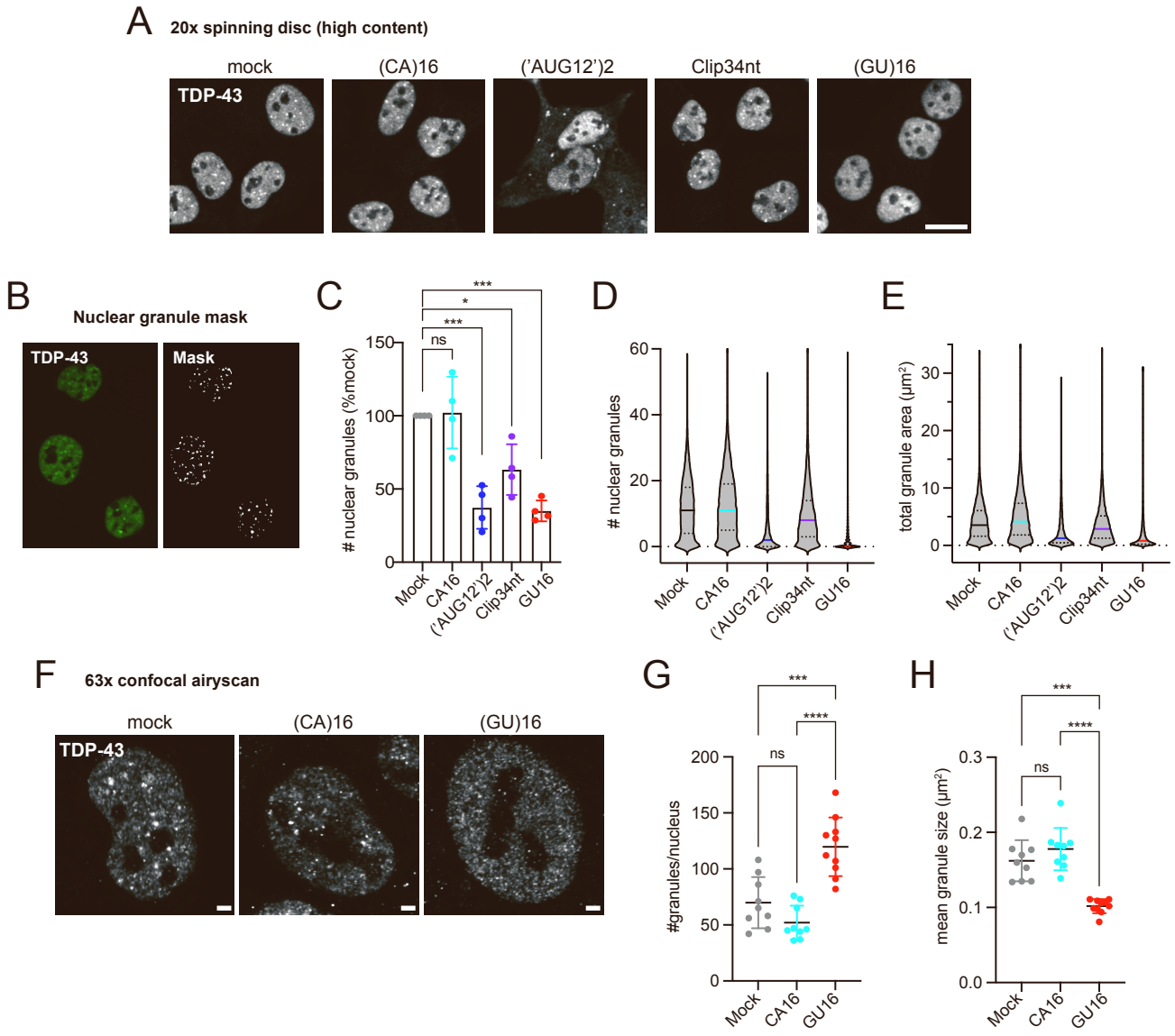

Figure S1. GU-oligonucleotide transfection alters nuclear TDP-43 granule morphology, related to figure 2. Oligo-transfected U2OS cells (125 nM, 24 h) were fixed and immunostained for TDP-43, and imaging/analysis of nuclear granule morphology was performed with 20x spinning disc high content microscope utilizing MetaXpress (**A-E**) or 63x confocal airyscan utilizing Image J (**F-H**). **A.** Representative 20x images. Scale bar = 20 µm. **B.** Representative nuclear granule mask generated with custom MetaXpress analysis module (lower limit 0.5 µm). **C.** Number of nuclear TDP-43 granules expressed as % mock-transfected cells. Mean ± SD of N=4 biological replicates. NS = not significant, *p<0.05, ***p<0.001 by one-way ANOVA with Tukey's post-hoc test. **D-E.** Violin plots of granule number (D) and total area/cell (E) from a representative replicate within C (n~4,000-12,000 cells per condition). Median, 25th, and 75th percentiles are indicated. **F.** Representative 63x confocal airyscan images. Scale bar = 2 µm. **G.** Mean number of TDP-43 granules/nucleus quantified by Image J 'analyze particles' function (lower limit 0.035 µm). **H.** Mean TDP-43 granule size (µm). In G-H, N=9-10 cells/group. NS = not significant, ***p<0.001, ****p<0.0001 by one-way ANOVA with Tukey's post-hoc test.

Figure S2

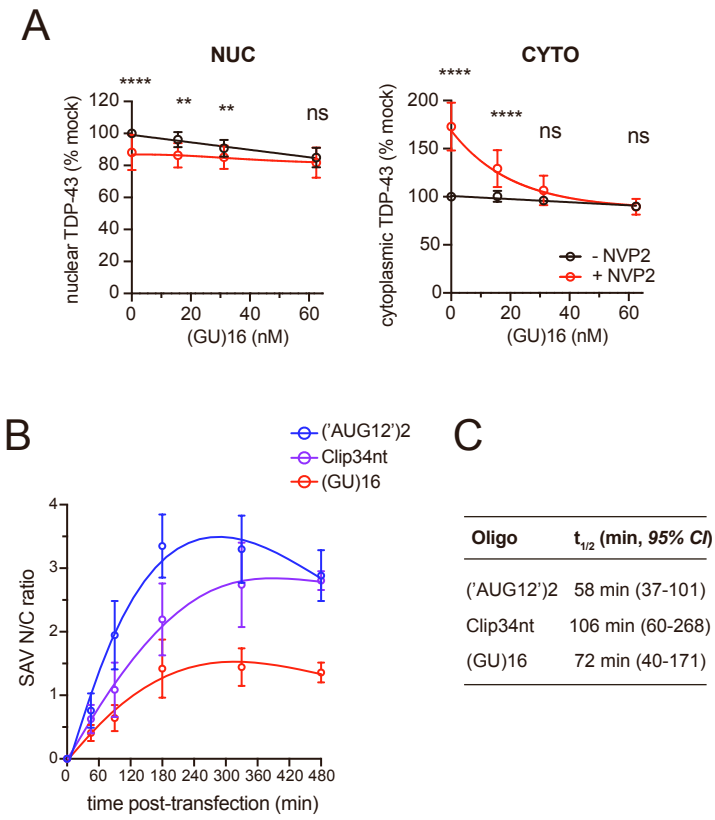

Figure S2. **Extended analysis, GU-oligo-induced nuclear TDP-43 retention, related to figure 3. A**. Nuclear and cytoplasmic intensity in (GU)16-transfected cells (% mock-transfected cells), with or without NVP2 treatment. These are the source data used to calculate the N/C ratios in fig 3C. Mean ± SD of n=15 biological replicates. NS= not significant, **p<0.01, ****p<0.0001 by 2-way ANOVA with Tukey's post-hoc test. **B.** SAV647 nuclear intensity in oligo-transfected cells during the NVP2 recovery assay in fig 3H-I. Mean ± SD from n=3 biological replicates. **C.** $t_{1/2}$ (min) for nuclear uptake calculated from (B) by non-linear regression. 95% CI is shown.

Figure S3

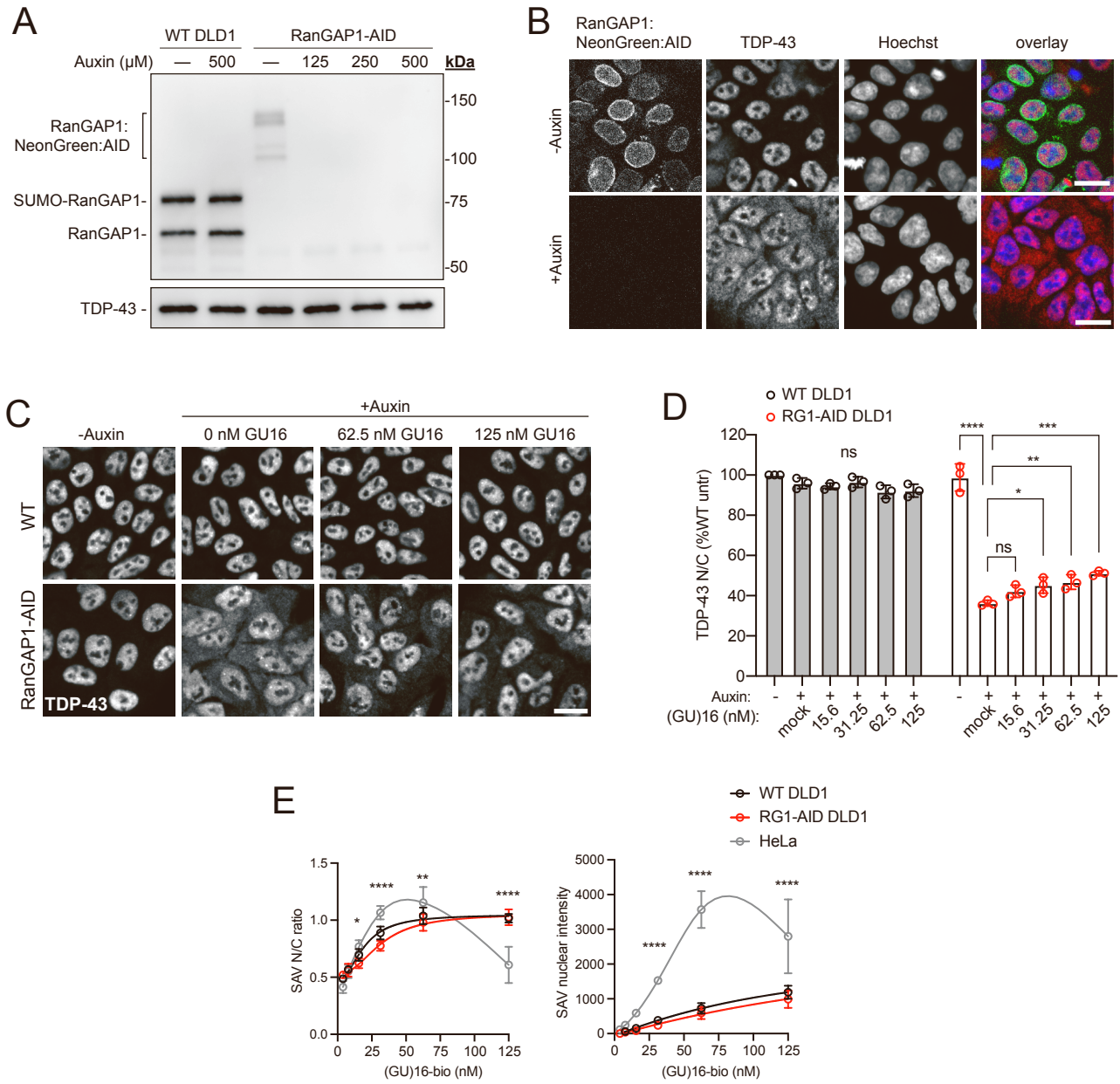

Figure S3. (GU)16 attenuates TDP-43 mislocalization in RanGAP1-auxin inducible degron (AID) cells, related to figure 3. **A.** RanGAP1 immunoblot in wild-type (WT) and RanGAP1-AID cells ± 2 h auxin (indoleacetic acid) treatment. Distinct bands were seen as expected for RanGAP1 and SUMOylated RanGAP1. Note: the RanGAP1 AID cell line has reduced RanGAP1 expression (bracket) suggesting accelerated RanGAP1 turnover independent of auxin (perhaps due to excess TIR1). TDP-43 expression is unchanged. **B.** Loss of RanGAP1:NeonGreen:AID epifluorescence in RanGAP1 AID cells after 2 h 500 μM auxin treatment is accompanied by cytoplasmic mislocalization of TDP-43 (immunostained with AF568-labeled secondary). Scale bar = 20 μm. **C.** TDP-43 immunostaining in WT versus RanGAP1 AID cells transfected with increasing concentrations of (GU)16 for 5 h followed by 2 h 500 μM auxin treatment. Scale bar = 20 μm. **D.** TDP-43 N/C expressed as %WT untreated cells. Mean ± SD from n=3 biological replicates. NS= not significant, *p<0.05, **p<0.01, ****p<0.0001 by 2-way ANOVA with Tukey's post-hoc test. **E.** SAV647 N/C ratio (left) and nuclear intensity (right) in biotinylated (GU)16-transfected DLD1 vs. HeLa cells under optimized conditions for each cell type. Mean ± SD for ≥3 biological replicates. *p<0.05, **p<0.01, ****p<0.001 by 2-way ANOVA with Tukey's post-hoc test (all groups were compared; asterisks are shown for HeLa vs. RG1-AID comparisons only).

Figure S4

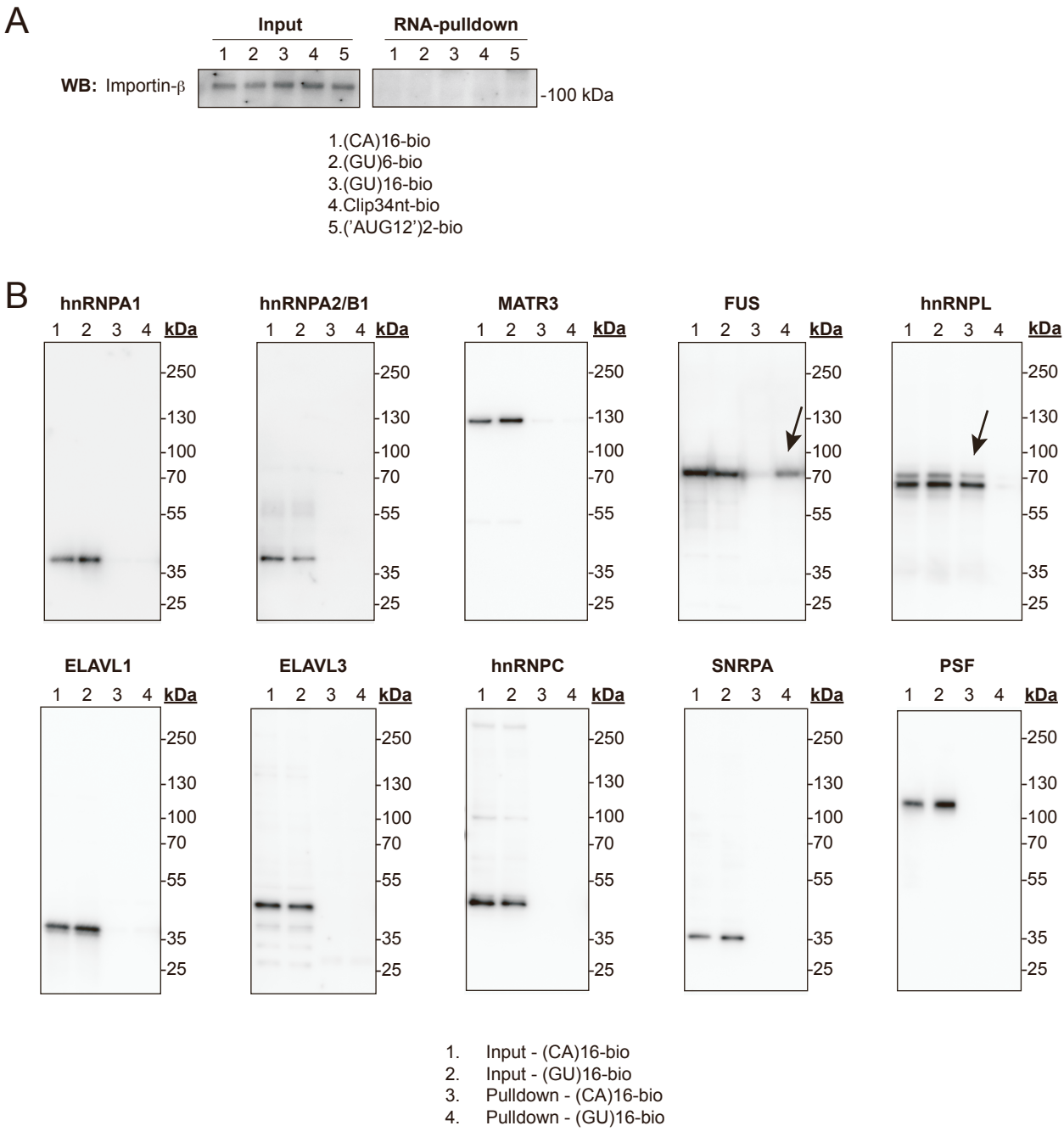

Figure S4. SAV-RNA pulldowns probed for additional binding partners, related to figure 4. SAV-RNA pulldowns from biotinylated oligo-transfected cells (62.5 nM, 5 h) that were UV crosslinked before lysis and probed with the indicated antibodies, to importin β (**A**), or a panel of nuclear RNA binding proteins (**B**). Note: the blot in A is a reprobe of the blot in fig 4a. Arrows in B indicate FUS binding to (GU)16 and hnRNPL binding to (CA)16.

Figure S5

Fig 1b

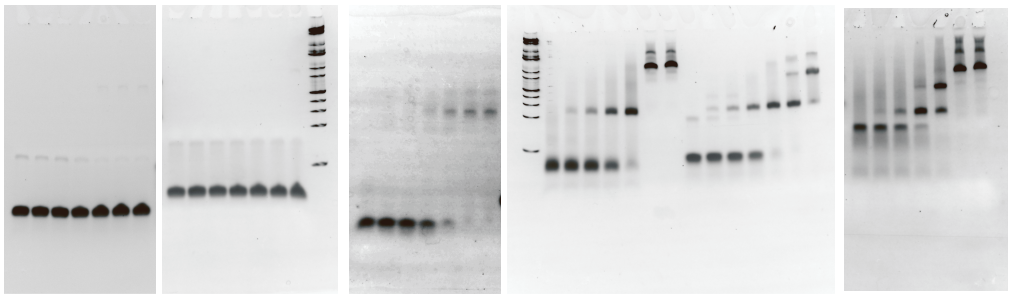

Fig 1d

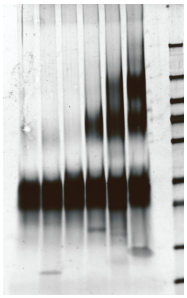

Fig 4a

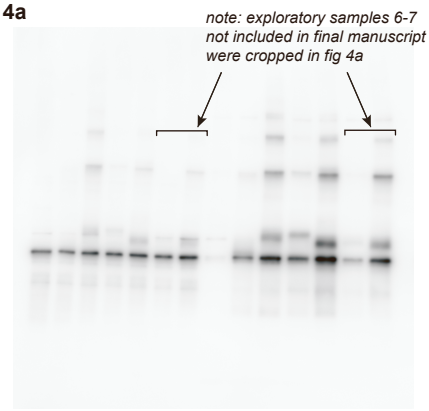

Fig 5e

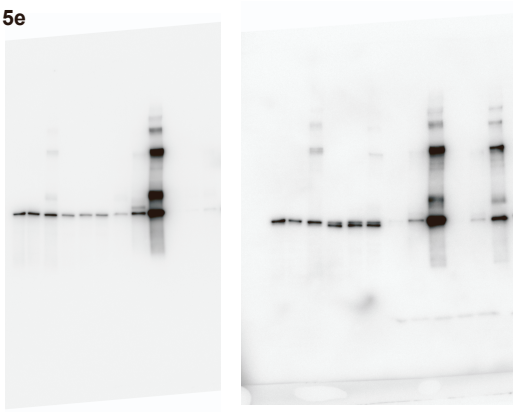

Fig 6a

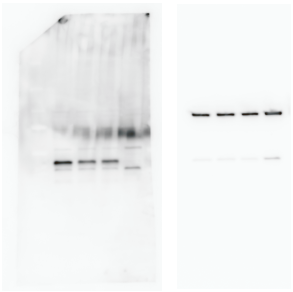

Fig 6b

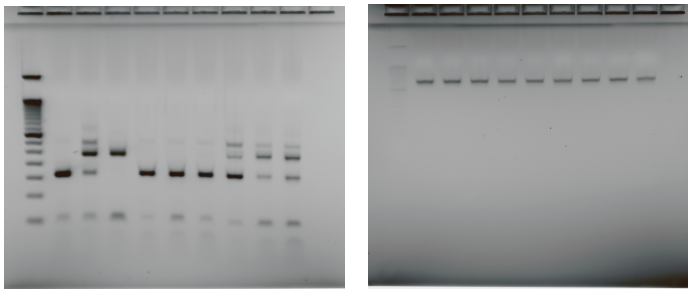

Figure S5. Unmodified gel images, related to figures 1, 4, 5, and 6.

SUPPLEMENTAL TABLES

Table S1. RNA oligonucleotides

Oligo	RNA sequence with modifications m: 2' O-methyl *: phosphorothioate bond	ID #
GU6-biotin	5'-mG*mU*mG* mU*mG*mU*mG*mU*mG* mU*mG*rU/3Bio/-3'	R78
GU16-biotin	5'-mG*mU*mG*mU*mG*mU*mG*mU*mG* mU*mG*mU*mG*mU*mG* mU*mG*mU* mG*mU*mG*mU*mG*mU*mG*mU*mG*mU*mG*mU*mG*rU/3Bio/-3'	R81, R102, R105
CA6-biotin	5'-mC*mA*mC*mA*mC*mA*mC*mA*mC*mA*mC*rA/3Bio/-3'	R75
CA16-biotin	5'-mC*mA*mC*mA*mC*mA*mC*mA*mC*mA*mC*mA*mC*mA*mC*mA*mC*mA* mC*mA*mC*mA*mC*mA*mC*mA*mC*mA*mC*mA*mC*rA/3Bio/-3'	R83, R107
('AUG12')2-biotin	5'-mG*mU*mG*mU*mG*mA*mA*mU*mG*mA*mA*mU*mG*mU*mG* mU*mG*mA*mA*mU*mG*mA*mA*rU/3Bio/-3'	R95
Clip34nt - biotin	5'-mG*mA*mG*mA*mG*mA*mG*mC*mG*mC*mG*mU*mG*mC*mA*mG*mA*mG* mA*mC*mU*mU*mG*mG*mU*mG*mG*mU*mG*mC*mA*mU*mA*rA/3Bio/-3'	R76, R103
A12-biotin	5'-mA*mA*mA*mA*mA*mA*mA*mA*mA*mA*mA*rA/3Bio/-3'	R74
A32-biotin	5'-mA*mA*mA*mA*mA*mA*mA*mA*mA*mA*mA*mA*mA*mA*mA*mA*mA*mA* mA*mA*mA*mA*mA*mA*mA*mA*mA*mA*mA*mA*mA*mA*rA/3Bio/-3'	R96

Table S2. Primers

Target	Sequence	Source or catalog #
RT-PCR		
EPB41L4A-F	GGACCTCCATATACTTTGTATTTTGGT	Tan *et al*., 2016
EPB41L4A-R	AGCTGAGCAGCAGTGTTGAC	Tan *et al*., 2016
GAPDH-F	ACCACAGTCCATGCCATCAC	IDT
GAPDH-R	TCCACCACCCTGTTGCTGTA	IDT
qRT-PCR		
EPB41L4A cryptic exon	F - ACATATGCACACACACTCTCACA Probe – CACTTCAGCCTGTCCTTT (FAM) R - AGTCACCTTACAAAACAGAAGTCACA	ThermoFisher custom assay APRWNHN
ARHGAP32 cryptic exon	F - CAGCCAAATGCACAGCGAAT Probe – AATGACCCAGTCAAAATA (FAM) R - GGAGGAAGCATTTTGGAGGTTTCTA	ThermoFisher custom assay APT2G3K